Changes in Interannual Tropical Atlantic–Pacific Basin Interactions Modulated by a South Atlantic Cooling

TERESA LOSADA,[a] BELÉN RODRÍGUEZ-FONSECA,[a,b] C. ROBERTO MECHOSO,[c] ELSA MOHINO,[a] AND ANTONIO CASTAÑO-TIERNO[a,d]

[a] *Departamento de Física de la Tierra y Astrofísica, Universidad Complutense de Madrid, Madrid, Spain*
[b] *Instituto de Geociencias, Consejo Superior de Investigaciones Científicas, Universidad Complutense de Madrid, Madrid, Spain*
[c] *Department of Atmospheric and Oceanic Sciences, University of California, Los Angeles, Los Angeles, California*
[d] *Instituto Español de Oceanografía, Madrid, Spain*

(Manuscript received 15 July 2021, in final form 11 March 2022)

ABSTRACT: Although tropical interbasin interactions at interannual time scales are presently receiving much attention, their controlling factors and variations on longer time scales are under debate. Tropical convection plays a crucial role in the occurrence and nonstationarity of them. In this paper, we investigate the dependence of interannual tropical Atlantic–Pacific basin interactions on convection-related features of the tropical oceans' climatology, especially the ITCZ position. We contrast a CGCM control simulation with an experiment in which tropical convection is modified by an artificial perturbation outside the tropics that reduces the incident shortwave radiation in a region of the South Atlantic. Based on previous work, this modification is expected to shift in latitude the climatological position of the simulated ITCZ. The experiment shows altered Walker circulations, stronger interannual variability over the tropical oceans, a westward extension of the Atlantic Niño pattern and of convection, and shallower thermocline in the Pacific, making the basin more sensitive to both local and remote perturbations. As a consequence, the experiment shows enhanced interannual Atlantic–Pacific basin interactions at the equator, and weaker teleconnections between the north tropical Atlantic and the equatorial Pacific. The latter seems to occur because the impact of the warm Atlantic SST anomalies is offset by the presence of warm SST anomalies in El Niño region. Despite the uncertainties raised because the simulations are relatively short, we conclude that this work presents a potential explanation for the long-term changes in the tropical basin interactions and offers a novel and useful methodology for their analysis.

KEYWORDS: Atmosphere-ocean interaction; Teleconnections; Climate models; General circulation models; Interannual variability

1. Introduction

Current seasonal forecast systems do a fair job in the prediction of ENSO (Zhang et al. 2017; Keenlyside et al. 2020). Nevertheless, further improvements would be extremely useful for seasonal prediction of climate variations that affect human activities. Recent works have put forward the notion that consideration of the tropical Atlantic variability can provide added value to the forecast skill of ENSO (Jansen et al. 2009; Frauen and Dommenget 2012; Martín-Rey et al. 2015; Cai et al. 2019; Keenlyside et al. 2020; Exarchou et al. 2021). Understanding the mechanisms controlling this remote impact from the Atlantic can help in the implementation of forecast system upgrades for better ENSO prediction.

In the tropical Atlantic the main mode of interannual variability is the so-called Atlantic Niño, which peaks in boreal summer (Zebiak 1993; Lübbecke et al. 2018). The Atlantic Niño can influence the main mode of interannual variability in the Pacific (ENSO) with a one-to-two season lag (Rodríguez-Fonseca et al. 2009; Ding et al. 2012; Rodríguez-Fonseca et al. 2020). This tropical interbasin connection is established through modification of the Walker circulation with enhanced rising motion above higher sea surface temperatures (SST) in the equatorial Atlantic and compensating increased sinking motion over the central Pacific (Rodríguez-Fonseca et al. 2009; Losada et al. 2010; An et al. 2020). The climate anomalies associated with such a change in the overturning circulation include stronger trades over the central equatorial Pacific, which trigger an upwelling oceanic Kelvin wave that initiates a La Niña event in the following winter (Polo et al. 2015). Such a special Atlantic Niño–ENSO teleconnection has been strong in the early decades of the twentieth century and after the 1970s, and either weak or undetectable in between (Martín-Rey et al. 2014). These nonstationarities in the Atlantic Niño–ENSO teleconnection have been associated with changes either in the background state of the SSTs (Martín-Rey et al. 2014) or even in the spatial pattern of the Atlantic Niño itself (Losada and Rodríguez-Fonseca 2016). The Atlantic multidecadal variability (AMV, previously referred to as AMO; Knight et al. 2005) has been put forward as potential modulator (Martín-Rey et al. 2018, 2019).

SST anomalies in the north tropical Atlantic (NTA, between 0° and 15°N, 80°W and 20°E) can also be precursors of an ENSO event. During boreal spring, positive SSTs can increase convection in the Atlantic component of the intertropical convergence zone (ITCZ; Ham et al. 2013a,b; Rodríguez-Fonseca et al. 2020).

Supplemental information related to this paper is available at the Journals Online website: https://doi.org/10.1175/JCLI-D-21-0546.s1.

Corresponding author: Teresa Losada, tlosadad@ucm.es

DOI: 10.1175/JCLI-D-21-0546.1

The associated changes in diabatic heating can trigger a Gill-type Rossby wave response whereby surface winds and local SSTs are modified in the eastern Pacific influencing the Pacific Niño occurrence (Ham et al. 2013b). According to these previous works, an equatorial Rossby wave triggered by positive SST anomalies in the NTA produces an anomalous cyclonic circulation in the off-equatorial eastern Pacific and an anomalous anticyclonic circulation to the west; the joint action of both of them produces strong easterly winds to the west and surface divergence and cooling of the central equatorial Pacific, inducing a central La Niña event (Ham et al. 2013a,b; Rodríguez-Fonseca et al. 2020).

Thus, two different connections between the tropical Atlantic and Pacific Oceans have been discussed: the Atlantic Niño–ENSO teleconnection, which has a more equatorial pathway and is established from boreal summer to boreal winter; and the NTA–ENSO connection, which follows an off-equatorial pathway and acts from boreal spring to boreal winter. Wang et al. (2017) showed that the latter teleconnection was active at the end of the twentieth century, after the year 1995, when the AMV changed to its positive phase. According to Wang et al. (2017), a positive AMV leads to a northward shift of the Atlantic ITCZ favoring the propagation of the tropical Rossby wave response to the NTA SST warming. A recent analysis of the observational record suggests that the NTA–ENSO teleconnection alternates in time with that between the Atlantic Niño and ENSO (Rodríguez-Fonseca et al. 2020).

According to the studies reviewed in the previous paragraphs, tropical Atlantic SST anomalies can result in local deep convection anomalies that alter the Atlantic–Pacific circulation activating a remote influence on ENSO. Changes in the background conditions of the Pacific should be also taken into account, as ENSO development can take place under small/big wind perturbations depending on the thermocline depth configuration (Fedorov and Philander 2000). Capturing such anomalies and connections poses major challenges to coupled atmosphere–ocean GCMs (CGCMs). These comprehensive tools for climate research must successfully simulate not only important processes internal to the atmosphere and ocean, but also coupling processes at the atmosphere–ocean interface. Current CGCMs, however, have persistent and systematic errors. In the tropical Pacific, for example, the simulated Pacific ITCZ often develops erroneously both north and south of the equator (Mechoso et al. 1995; Oueslati and Bellon 2015; Adam et al. 2018; Tian and Dong 2020; among other papers). In the Atlantic, the ITCZ is overestimated south of the equator (Richter et al. 2014; Mohino et al. 2019). Errors are particularly strong in the southeastern oceans, where the simulated SSTs are too warm in most models (Wang et al. 2014) and stratocumulus decks are usually underestimated (Ma et al. 1996; Yu and Mechoso 1999; Richter 2015).

Much work has been dedicated to the analysis of systematic CGCMs errors, and particularly to the poor representation of the ITCZ. One line of research on this topic has looked for the impact on the ITCZ and other features of the tropical climate of perturbations to hemispheric heating that are asymmetric about the equator (Broccoli et al. 2006; Chiang and Friedman 2012; Friedman et al. 2013; McGee et al. 2018; among others).To examine the links between CGCM errors in simulations of the tropical climate and of the interhemispheric difference in net energy input into the atmosphere represented by too-high SSTs over the Southern Ocean, Mechoso et al. (2016; hereafter M16) performed an idealized experiment with two CGCMs in which the latter errors were reduced by application of an artificial perturbation. This consisted of reducing the incident shortwave (SW) radiation at the top of the atmosphere in a latitude band from 60° to 30°S. A broader exploration of this concept was carried out under a community effort known as Extratropical–Tropical Interaction Model Intercomparison Project (ETIN-MIP; Kang et al. 2019), which contrasted long simulations by different CGCMs in which a similar SW reduction was imposed at different latitude bands (Kang et al. 2019). All the above experiments obtained a shift of the ITCZ to the warmer hemisphere (i.e., the hemisphere in which the perturbation was not applied) as the Hadley cell increased the energy transport to the cooler hemisphere (Kang et al. 2008; 2009; Broccoli et al. 2006; Kang et al. 2019). Moreover, ocean dynamics acted to damp the ITCZ response (Green and Marshall 2017; Xiang et al. 2018; Yu and Pritchard 2019; Green et al. 2019). The tropical response obtained proved sensitive to the location and strength of the extratropical energy forcing (Xiang et al. 2018; White et al. 2018; Kang et al. 2019). Interpretation of the results of such experiments has been aided by conceptual studies on the mechanisms determining the ITCZ shifts due to extratropical energy perturbations (Broccoli et al. 2006; Kang et al. 2008, 2009; Kay et al. 2016; Green and Marshal 2017; Kang 2020, and references therein).

To our knowledge however, no published study on the influence of interhemispheric heating differences on the tropical climate in CGCMs has addressed the issue of how the simulated interannual variability in the tropics is affected. If such an influence occurs, then a natural follow up issue is whether the interbasin connections among the modes of tropical variability are modified. In the present work, we address the tropical interannual variability issue by analyzing idealized experiments performed with a CGCM in which the incoming solar radiation in the Atlantic sector of the SO is reduced. We will start by showing that our perturbed simulation, although being less realistic in terms of incoming solar radiation, is better than the control in terms of location of the ITCZ. It is worth noting that we are not interested in improving the global performance of the model, but in understanding the physical mechanisms controlling the tropical Atlantic–Pacific teleconnections. Thus, being able to perturb the position of the regions of tropical convection in the model without directly interfering with the simulation in the tropics is advantageous for our purposes. We will show that the interannual variability of a control simulation is enhanced by the perturbation of the experimental setup described above. Next, we will focus on the alteration of the interbasin connections.

The work is organized as follows: The GCM, simulations performed, and methods of analysis are described in section 2. Section 3 contains the main results of the work regarding the changes in the mean state of the climate. The changes in interannual variability are explained in section 4. Finally, the summary and conclusions are presented in section 5.

2. Model and experiments

Our coupled atmosphere GCM is identical to the model used in M16. The atmospheric component of this model is the University of California, Los Angeles (UCLA) AGCM, version 7.1 (Mechoso et al. 2000; Ma et al. 2013), which has a sigma vertical coordinate system up to 1 hPa, with 29 layers (15 in the troposphere), a horizontal resolution of 2° latitude × 2.5° longitude and incorporates the Simplified Simple Biosphere Model (SSIB; Xue et al. 1991). The oceanic component is the Massachusetts Institute of Technology (MIT) OGCM (Marshall et al. 1997), covering the ocean domain from 80°S to 79°N. The OGCM version has 46 vertical levels to a maximum depth of 5815 m; the first OGCM level is at 5-m depth and levels are 10-m depth apart up to 155 m. In longitude, the resolution is 1°; in latitude the resolution is 0.3° between 10°S and 10°N, increasing up to 1° out of the tropics. The UCLA AGCM is especially sensitive to stratocumulus–SST feedbacks (M16).

Our experimental design modifies the approach in M16 and Kang et al. (2019). In these studies, the SW radiation incident at the top of the atmosphere is artificially reduced in full latitude bands. In the present work, the SW radiation is reduced between 60° and 30°S and between 60°W and 30°E, that is, over the South Atlantic sector (black box in Fig. 1a). We have several reasons for this strategy. First, the warm bias shown by global models in the Southern Ocean is not homogeneous in longitude, having the highest values over the Atlantic–Indian sector (see Fig. 1 in Wang et al. 2014). Second, the southern extratropical changes related to the Atlantic multidecadal variability have stronger loadings in the Atlantic sector (Fig. S1 in the online supplementary material). Third, M16 aimed to assess sensitivity to perturbation rather than better model performance. In this regard, we verified a posteriori that, when cooling with a similar magnitude is applied on the entire latitude band of the Southern Ocean, the simulated tropical climate has some unrealistic features, such as a too cold equatorial Pacific and an unrealistically strong northward shift of the tropical convection over the equatorial Pacific (not shown).

We will refer to our simulation with reduced SW radiation at the top of the atmosphere restricted to the Atlantic sector as AtlSim. The results of AtlSim are compared with those of a control simulation (CTL). The AtlSim and CTL are 96 and 85 years long, respectively, of which the first 35 years in both cases were discarded. Hence, the lengths of CTL and AtlSim analyzed are 50 and 61 years, respectively. In the following sections, results are shown in terms of differences between AtlSim and CTL and of regressions of different variables on two indices: 1) boreal summer Atl3 [SST averaged between 3°S and 3°N and between 20°W and 0° in June–September (JJAS); blue box in Fig. 1], and 2) boreal spring NTA (SST averaged between 0° and 15°N and between 80°W and 20°E in

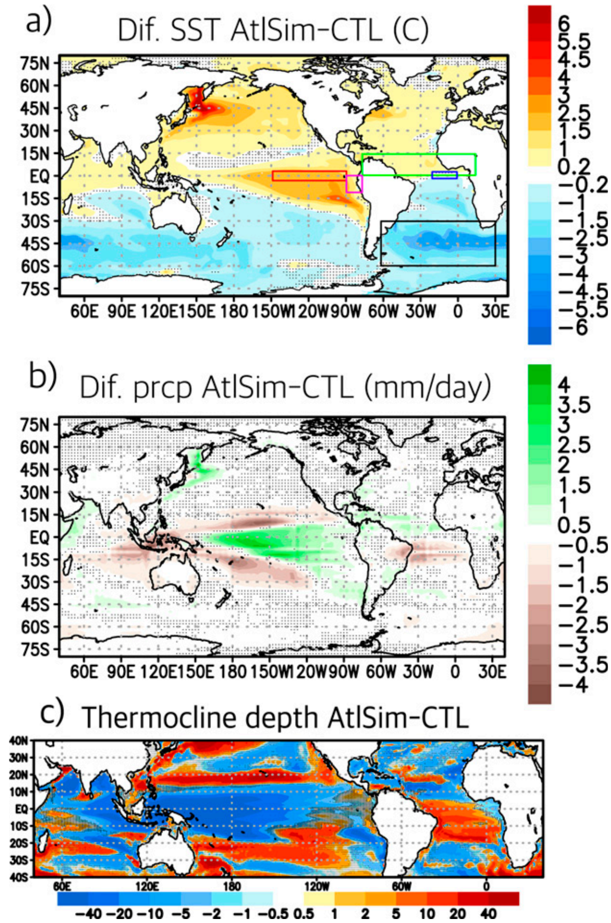

FIG. 1. Differences in annual (a) SST (°C), (b) precipitation (mm day^{-1}), and (c) thermocline depth (m) in AtlSim with respect to CTL. Not-dotted regions show significant differences at the 95% level. Boxes in (a) denote the regions for the incoming SW reduction (black), Atl3 index (blue), NTA index (green), Niño-3 index (red), and Niño-1+2 index (magenta). Positive (negative) values in (c) mean deeper (shallower) thermocline for AtlSim.

MAM; green box in Fig. 1). Labeling of seasons follows those of the Northern Hemisphere throughout the manuscript.

To remove any decadal variability that may be masking the results, we applied a high-pass Butterworth filter to remove low-frequency variability with periods longer than 7 years. Also, to remove the influence of previous winter ENSO on NTA and Atl3 variability we remove the linear regression with respect to the previous winter Niño-3 index (SST averaged between 5°S and 5°N and between 150° and 90°W, red box in Fig. 1) from the NTA and Atl3 index, following Ham et al. (2013a). Applying this preprocessing, however, would not remove the nonlinear effect of decadal variability of the background state on ENSO, or intrinsic random interannual variability. Thus, the relatively shortness of the simulations can make it difficult to separate the interannual forced signal. To partially overcome this, the significance of the regressions is estimated using the more restrictive Ebisuzaki random phase test (Ebisuzaki 1997), which is a nonparametric test

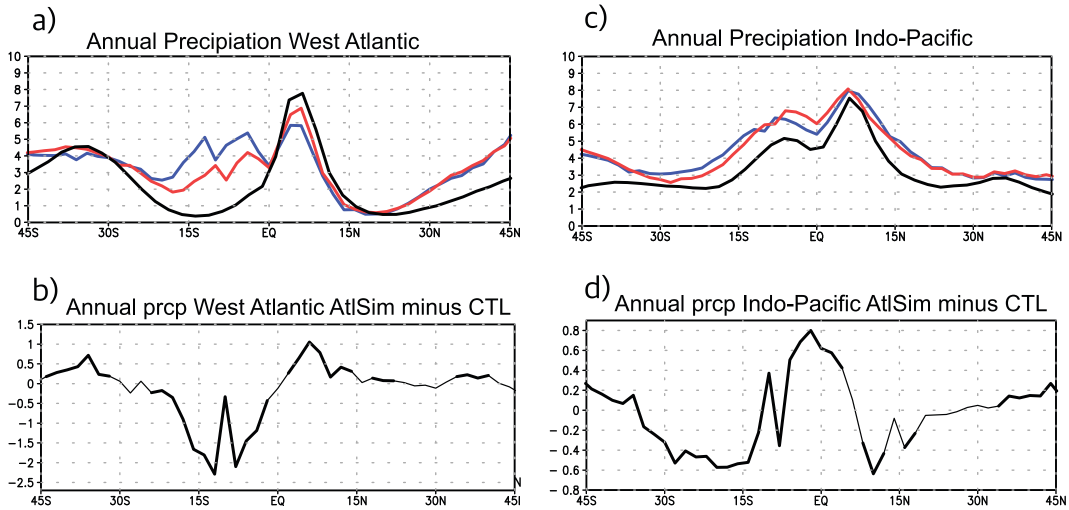

FIG. 2. Annual mean precipitation (mm day^{-1}) zonally averaged over the (a) west Atlantic (35°–15°W) and (c) Indo-Pacific (40°E–60°W) sectors for the observations (black line), AtlSim (red line), and CTL (blue line). Difference between AtlSim and CTL precipitation for the (b) west Atlantic and (d) Pacific sectors. Black thick lines show the significant regions at the 95% level.

designed to consider the autocorrelation of time series. We perform the Ebisuzaki test with 200 permutations. To assess the significance of the differences in regressions between simulations, a t test of regression slope has been performed. Finally, an F test has been used for the ratio of variances. All model results shown are estimated as to be at the 95% significance level except otherwise stated.

3. Change in the simulated tropical climate

Previous works (Martín-Rey et al. 2014, 2018, 2019; Losada and Rodríguez-Fonseca 2016; Wang et al. 2017; Rodríguez-Fonseca et al. 2020) have suggested two candidates for the multidecadal variations in the Atlantic Niño–ENSO teleconnection: 1) changes in the background state of the system (i.e., modifications due to multidecadal variability and/or climate change), and 2) changes in the characteristics of the Atlantic Niño mode. According to previous results (Wang et al. 2017; Rodríguez-Fonseca et al. 2020), changes in the climatological state of the system are also of critical importance in the characteristics of NTA–ENSO connection. Next, we take a closer look to these two factors for a better understanding of the model responses to the perturbation that was prescribed.

a. Changes in the mean state of the atmosphere and ocean

The model captures the seasonal cycle and variability of the tropical Atlantic and Pacific Oceans represented by the Atl3 and Niño-3 (SST averaged between 5°S and 5°N and 150° and 90°W) mean and standard deviation indices for both CTL and AtlSim (see Fig. S2 in the supplementary material). For the NTA index, the simulated mean seasonal cycle agrees well with the observations, but the variability is delayed by 2–3 months (Figs. S2c, f).

In reference to CTL, reducing the incoming shortwave radiation over the Atlantic sector of the Southern Ocean produces an SST cooling in the whole extratropical Southern Hemisphere, except near the equator in the Pacific (Fig. 1a). Conversely, the extratropical Northern Hemisphere becomes warmer with maxima in the westernmost part of both oceans. In the tropics, a warming takes place in the region in which the Pacific ENSO develops accompanied by a cooling in the tropical South Atlantic toward the equator.

According to previous studies (see the introduction section), a south–north interhemispheric gradient in Atlantic SST would produce a northward shift of the ITCZ and a reduction of the double ITCZ in the simulated climate. This is the case for the Atlantic sector (Fig. 1b), in which precipitation anomalies show a dipole with positive (negative) values to the north (south). In the tropical Pacific, the response of the rainfall around the date line shows a tripolar configuration, with precipitation enhanced at the equator and weakened poleward of it. AtlSim also shows a weakening of the SPCZ and an equatorial shift of the Pacific ITCZ, the combined action of which lead to the narrowing of the Pacific ITCZ. This narrowing, together with the reduction of precipitation over the Maritime Continent, is consistent with a modification of the Pacific cell of the Walker circulation similar to the one during an El Niño event in the Pacific, in which the upward motion is shifted to the east.

To highlight the different characteristics of the ITCZ in the west equatorial Atlantic in AtlSim and CTL, we compare the annual average of the precipitation averaged between 35° and 15°W in our simulations and in the observations (CMAP precipitation dataset; Xie and Arkin 1997), following Chiang et al. (2002). CTL (Fig. 2a, blue line) clearly overestimates the Atlantic precipitation in the southern tropics and underestimates it in the northern tropics south of 15°N (Fig. 2a, blue

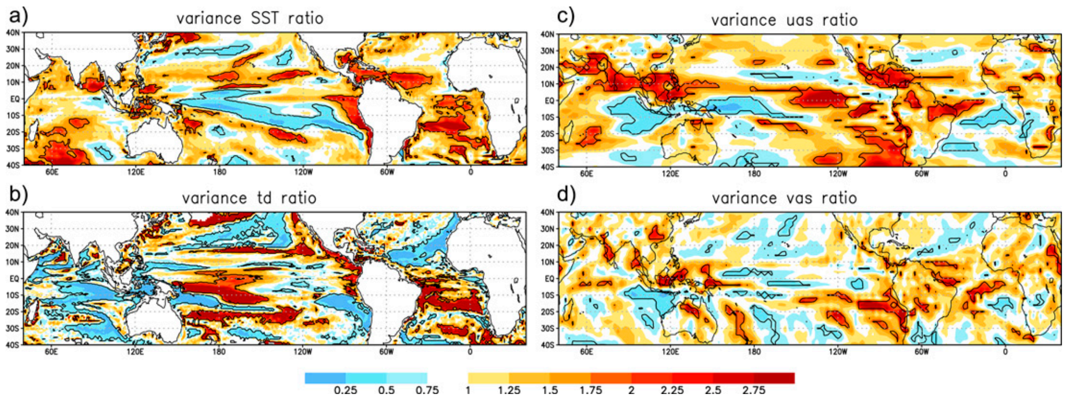

FIG. 3. Ratio of the annual variance of (a) SST, (b) thermocline depth, (c) surface zonal wind, and (d) surface meridional wind between AtlSim and CTL. Black contours denoted regions where the ratio is significant at the 95% with an F test.

line). A combination of these effects results in a strong peak of precipitation between 15°S and the equator with almost equal amplitude than the peak north of the equator. Reducing the incoming SW radiation in the Atlantic sector of the Southern Hemisphere results in a strong weakening of the spurious southern peak and an enhanced northern peak (Fig. 2a, red line), with maximum value located about two degrees north with respect to CTL (6° and 4°N, respectively). This implies a significantly more realistic simulation of the tropical Atlantic ITCZ that could be related to the warming in the equatorial Pacific and the south–north gradient of Atlantic SST (Chiang et al. 2002). Over the Indo-Pacific (40°E–60°W) ITCZ, the equatorial narrowing in AtlSim is clear, with precipitation enhanced within the band 7°S–7°N, and reduced outside this band (Figs. 2c,d). Following Adames and Wallace (2017), such changes can also be related to the ENSO-like SST pattern in the tropical Pacific.

Thus, the changes in the characteristics of the ITCZ (Figs. 1b and 2) in AtlSim with respect to CTL can be explained by the changes in the background SST (Fig. 1a).

Next, we examine the changes in the ocean circulation by looking at the tropical Atlantic thermocline depth, which is a key factor controlling the variability of the equatorial Atlantic (Zebiak 1993; Martín-Rey et al. 2018, 2019). Following Castaño-Tierno et al. (2018), we define thermocline depth as the depth at which the vertical ocean temperature gradient is maximum. As depicted in Fig. 1c, the Atlantic thermocline around the equator in the AtlSim is deeper than in CTL in the western part of the basin, and shallower in the eastern part. This is consistent with an enhanced total wind stress in the equatorial Atlantic (Fig. S3, supplementary material) that contributes to the ocean mixing, thus impacting the thermocline depth in the west. At this point we hypothesize that the theoretical modes described by Fedorov and Philander (2000) for the equatorial Pacific can be extrapolated to the equatorial Atlantic. According to Fedorov and Philander (2000), under a background state with a deeper thermocline in the west, dynamical feedbacks can develop if stronger winds are imposed at the ocean's surface. This is the case of the equatorial Atlantic in AtlSim, in which a deeper thermocline than in CTL is related to enhanced east–west SST gradients (Fig. 1a) and stronger easterly equatorial winds (Fig. S3, supplementary material). Thus, the changes in the background state of the Atlantic in AtlSim are consistent with the Atlantic being more sensitive to variations of the wind stress and, thus, more prone to produce enhanced variability in this ocean (Martín-Rey et al. 2018). This is confirmed by the higher variance ratio of the annual SST (Fig. 3a), Atlantic thermocline depth (Fig. 3b) and surface winds (Figs. 3c,d) between AtlSim and CTL. It is well known that the zonal wind stress in the western part of the basin has a major role in the Bjerknes feedback (Bjerknes 1969), so it is expected that a higher variability in the surface wind, such as the one shown in Fig. 3c for the Atlantic, will produce a higher variability in the Atlantic thermocline depth (Fig. 3b), as well as in the SST over the central and eastern equatorial Atlantic (Fig. 3a). The shallower thermocline in the eastern Atlantic has a weaker variability. Overall, the patterns of enhanced variability in the Atlantic in AtlSim with respect to CTL that are shown in Fig. 3, roughly agree with a strong dynamical coupling through the Bjerknes feedback as described in previous literature (Deppenmeier et al. 2016) and could be consistent with observed changes in the Atlantic Bjerknes feedback at decadal time scales as those described in Dippe et al. (2019).

The differences in thermocline tilt and depth are also outstanding in the tropical Pacific (Fig. 1c). In AtlSim the thermocline is shallower and flatter than in CTL, which is consistent with the El Niño–like state shown in Fig. 1a. Zhu et al. (2015) found that a shallower thermocline in the equatorial Pacific produces a stronger link in the wind–SST–thermocline feedback. We find a similar result in our simulations, in which the annual correlation between SST and thermocline depth in Niño-3 region increases from 0.12 in CTL to 0.30 (significant at the 95% level) in AtlSim. We also find that the equatorial Pacific stratification is stronger in AtlSim than in CTL (Fig. S4, supplementary material), which facilitates wave propagation. The change in the Pacific thermocline slope and

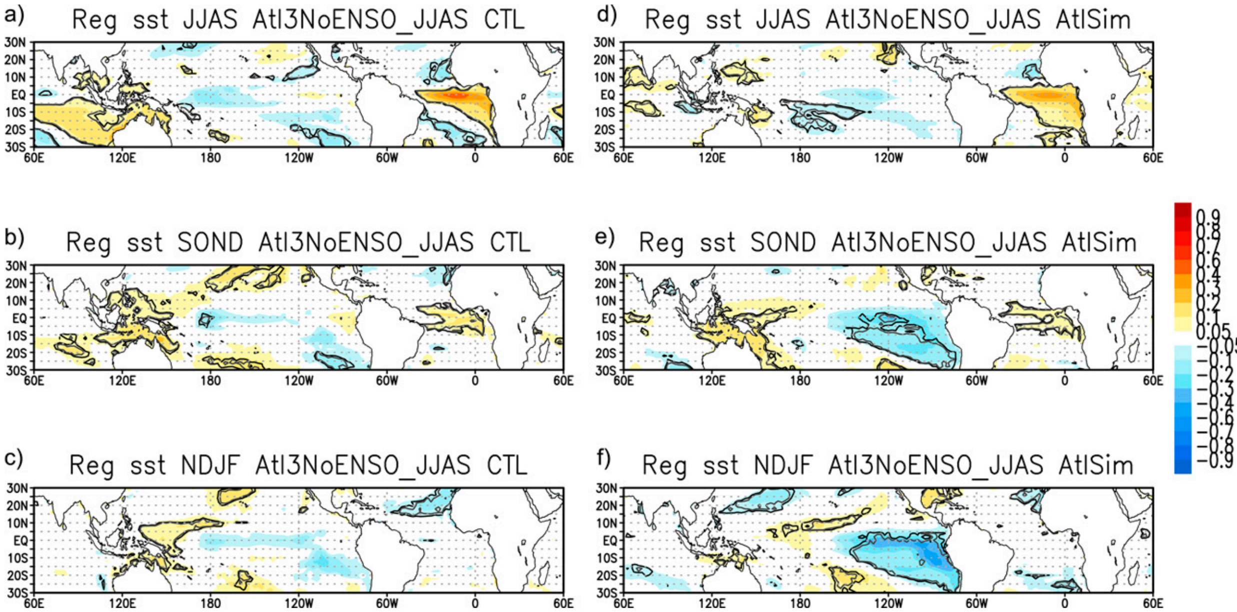

FIG. 4. Regressions of the (a),(d) JJAS, (b),(e) SOND, and (c),(f) NDJF SST (°C) onto the JJAS Atl3 index for (left) CTL and (right) AtlSim. Gray (black) contours show significant correlations at the 95% (90%) level.

in the stratification found in AtlSim would lead to increased ENSO variability (Hu et al. 2013), enhancing the response of the equatorial Pacific to atmospheric perturbations. Thus, the characteristics of the Pacific upper ocean in AtlSim would make the equatorial Pacific more sensitive to atmospheric perturbations. These results agree as well with Fedorov and Philander (2000), who discussed ENSO development depending on the ocean and atmospheric background conditions finding that, when the thermocline is shallower (as it is the case for the Pacific in AtlSim compared to CTL), small perturbations in the western equatorial Pacific are enough to trigger the development ENSO. We also find that the ENSO period changes from 4 years in CTL to 2.5 years in AtlSim. This feature also agrees with Fedorov and Philander (2000), who showed that ENSO's periodicity can decrease for a background state with a shallower thermocline and weaker winds in the west. The configuration of the variability in the Pacific is consistent with the dynamical response of the ocean to a wind anomaly described by Neelin (2010): the variability in the equatorial wind will induce variability of the thermocline centered at the equator to the east of the wind anomaly, and north and south of the equator to the west; then, the variability in the eastern thermocline will induce variability in the eastern SST, which, in turn, will affect the variability of the winds, closing the loop. Moreover, the weakening of the SST zonal gradient in the equatorial Pacific in AtlSim with respect to CTL (Fig. 1a) would be consistent with prevalence of eastern Pacific ENSO events (Wang et al. 2019), which show higher frequency than central ones (An and Wang 2000). The regression of AtlSim SST onto November–February (NDJF)–Niño-3 shows ENSO events with stronger SST loadings at approximately 140°W, consistent with moderate eastern Pacific ENSO events described by Wang et al. (2019), and with larger amplitude and frequency than ENSO events from CTL (not shown).

The changes in the climatological state from CTL to AtlSim show a narrower and strengthened equatorial ITCZ in the Atlantic and Pacific, enhanced variability in the equatorial Atlantic and a shallower and flatter thermocline in the equatorial Pacific that produce enhanced variability and frequency of ENSO. Taken together, all these factors can result in a modification of tropical Atlantic–Pacific connections, which will be examined in section 4.

b. Differences in the Atlantic El Niño in CTL and AtlSim

Let us next consider the SST anomalies associated with a positive Atl3 index in both AtlSim and CTL simulations. To do this, we examine the Atlantic pattern obtained by regressing the simulated SST anomalies onto the high variability Atl3 index in boreal summer (JJAS) and in the following boreal fall (SOND) and winter (NDJF). We perform this regression with the Alt3 index removing the previous winter ENSO signal (Fig. 4) and without removing it (Fig. S5, supplementary material).

For both regressions, boreal summer anomalies have stronger amplitudes in the eastern part of the Atlantic basin in CTL, but their geographical extent is larger in AtlSim with positive values reaching westward toward the American coast (Figs. S5a,d). The differences between the Atlantic patterns in Fig. S5 and Fig. 4 are high. When the previous ENSO signal is not removed, the Atlantic Niño appears together with strong anomalies in the NTA region. Such anomalies disappear when the previous year ENSO is linearly removed. Since this work aims to study the impacts of equatorial Atlantic and NTA separately, we decide to perform the rest of the analysis using the Atl3 index removing the previous year ENSO. Although the differences in the Atlantic Niño pattern between CTL and AtlSim are weaker when ENSO is removed, they still exist, becoming clearer when looking at the differences between the two regressions, which show a westward displacement of the maximum anomalies in AtlSim and warmer SSTs in the coast of South America (Fig. S6). Losada and Rodríguez-Fonseca (2016) described an observed change in the Atlantic Niño pattern in the period 1975–94 with respect to 1950–70, which resembles the one found in AtlSim with respect to CTL. In that work, they concluded that the westward extension of the Atlantic Niño leads to a westward shift of the associated Atlantic deep convection, which, in turn, produces a stronger impact in the equatorial Pacific Ocean, enhancing the equatorial Atlantic–ENSO teleconnection.

As a measure of low-level convergence and deep convection in the tropics, we compute boreal summer regression of the moist static energy (MSE) in the planetary boundary layer (PBL) onto the Atl3 index in both CTL and AtlSim (Fig. 5). In the CGCM we are using, the PBL is parameterized as a well-mixed layer of variable depth (Li et al. 2002) that is predicted through the mass budget equation including the PBL-top entrainment, cumulus mass flux, and horizontal mass convergence within the PBL (Konor et al. 2009). The regression of the MSE onto the boreal summer Atl3 index shows positive MSE anomalies that are stronger and cover the entire equatorial ocean basin in AtlSim. This leads to a more unstable atmosphere in AtlSim than in CTL over the equatorial Atlantic, especially west of 40°W and in the Amazonian convective region, where the differences between regressions are larger (Fig. 5c). Thus, AtlSim shows more favorable conditions for convection over the western equatorial Atlantic, which can alter the Atlantic–Pacific Walker circulation leading to a stronger impact on the equatorial Pacific, in agreement with previous works (Rodríguez-Fonseca et al. 2009; Losada et al. 2010; Polo et al. 2015; Losada and Rodríguez-Fonseca 2016). This will be further analyzed in section 4.

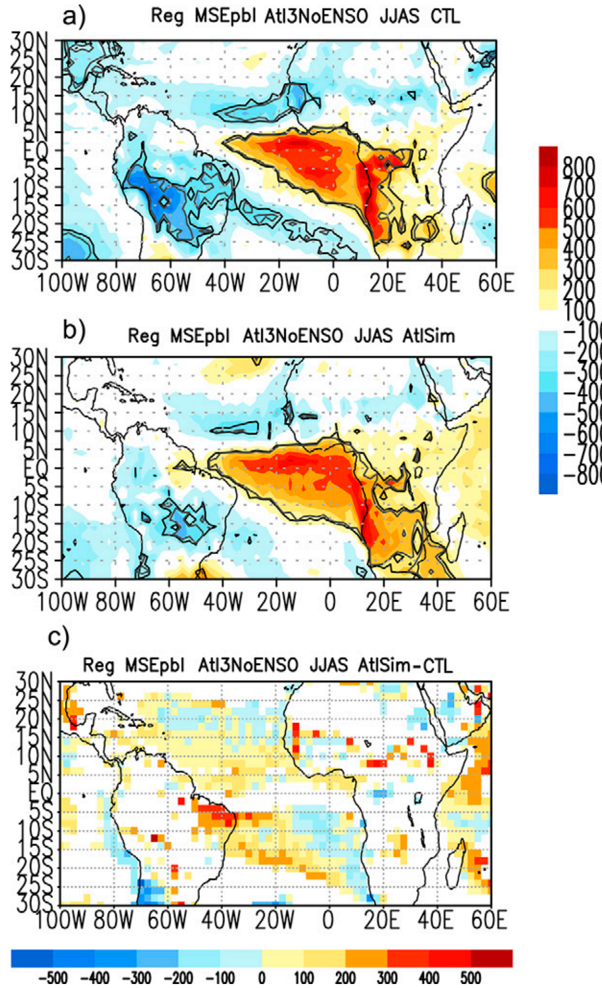

FIG. 5. Regression of the JJAS MSE in the PBL ($m^2 s^{-2}$) onto the JJAS Atl3 index for (a) CTL and (b) AtlSim. Gray (black) contours show significant correlations at the 95% (90%) level. (c) Significant differences between (a) and (b) at the 95% level.

4. Changes in the tropical interbasin teleconnections

a. Atlantic Niño–ENSO teleconnection

We move on to examine the model's performance in representing the influence of tropical Atlantic on the tropical Pacific variability. To do this we regress simulated SST anomalies onto the high-variability Atl3 index for boreal summer (JJAS) and for the following boreal autumn (SOND) and winter (NDJF). To rule out the possibility of a Pacific Niño-to-Atlantic Niño relationship, as the one described by Tokinaga et al. (2019) and Rodrigues et al. (2011), we remove from the Atl3 index the previous winter Niño-3 signal with a linear regression, following the methodology used by Ham et al. (2013a).

No significant relationship is found in CTL between boreal summer equatorial Atlantic variability and next winter Pacific ENSO (Figs. 4a–c). The picture is different in AtlSim, for which the regressions show that a La Niña tends to develop in the Pacific six months after an Atlantic Niño event (Figs. 4d–f). Moreover, the correlation coefficient between JJAS–Atl3 and NDJF–Niño-3 increases in magnitude from −0.04 in CTL to −0.22 (significant at the 90% level) in AtlSim. As Fig. 4 shows that the relationship between Atl3 and tropical Pacific SSTs is stronger over the eastern Pacific than over the central Pacific, we look at the correlations between JJAS–Atl3 and NDJF–Niño-1+2 (SST-averaged anomalies in the region 0°–10°S, 90°–80°W, magenta box in Fig. 1). These correlations change from 0.02 in CTL to −0.28 in AtlSim (significant at the 95% level). Our simulations are 50 and 61 years long. Multidecadal variability within each of the simulations may modulate the correlation between interannual indices, which makes difficult to extract the forced signal in simulations of this length. Thus, even though the changes between the background states from CTL and AtlSim are very large and suggest that any multidecadal variability within each simulation will be of smaller order when compared with the changes between simulations, the results that we present

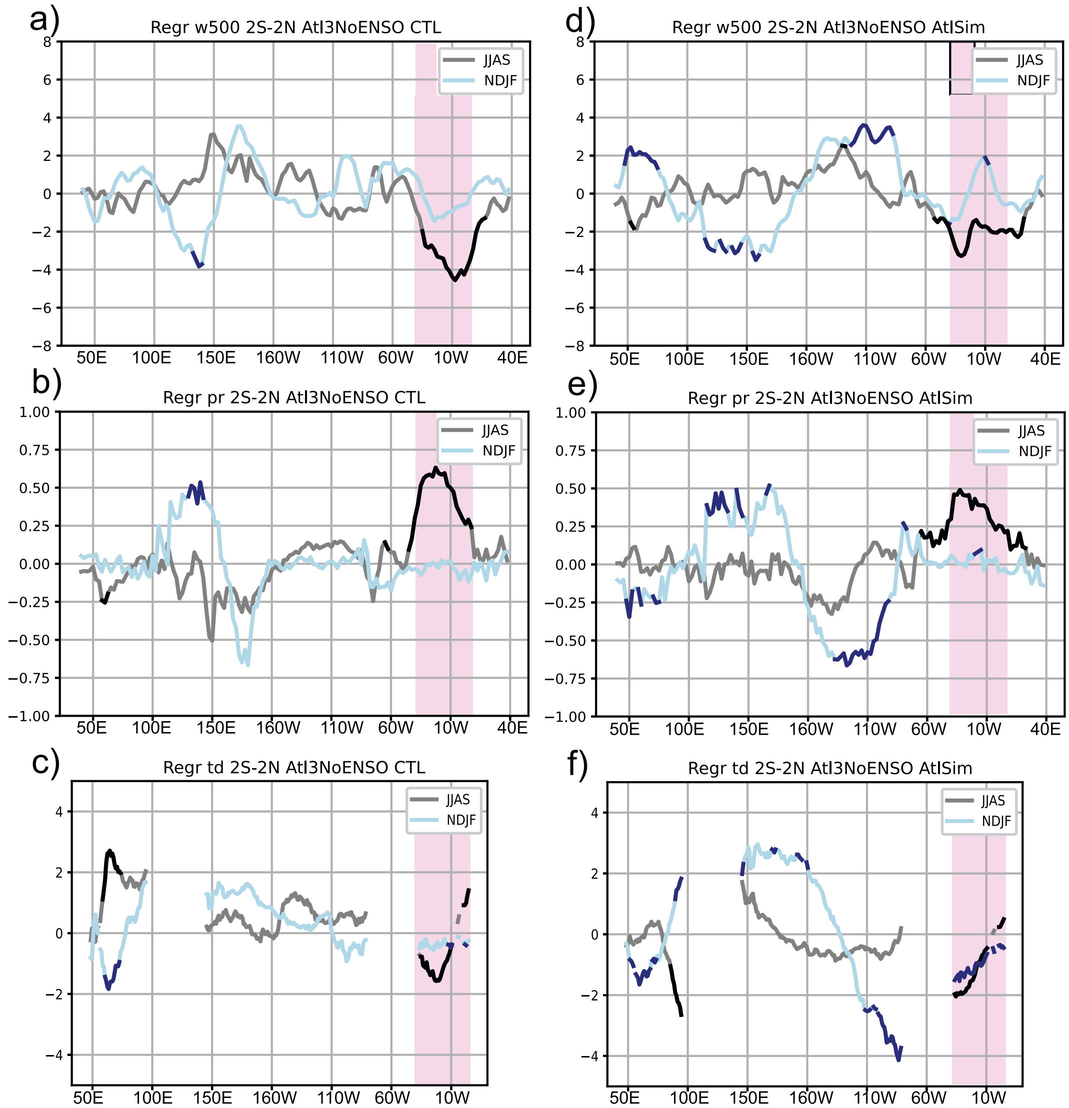

FIG. 6. Regression of the JJAS (gray line) and NDJF (light blue line) 2°S–2°N (a),(d) averaged omega at 500 hPa (Pa s^{-1}), (b),(e) precipitation (mm day^{-1}), and (c),(f) thermocline depth (m) onto the JJAS Atl3 index for CTL simulation in (a)–(c) and AtlSim in (d)–(f). Black and dark blue lines denote statistically significant correlation at a 95% level for JJAS and NDJF regressions, respectively. The Atlantic Ocean region is showed in light magenta shading. Positive (negative) values in (c) and (f) mean deeper (shallower) thermocline related to positive Atlantic Niño events.

hereafter should be viewed while keeping in mind this signal-to-noise issue. Regressions of different atmospheric and oceanic variables onto boreal summer Atl3 index (Fig. S7, supplementary material) suggest an altered Pacific Walker circulation in boreal summer, with anomalous convergence of surface winds over the equatorial Atlantic and divergence over the equatorial Pacific around 150°W, with shallower thermocline in the eastern Pacific and an eastern La Niña event the winter following an Atlantic Niño. The patterns in Fig. S7 closely resemble those obtained by Polo et al. (2015) using results from Simplified Parameterizations Primitive Equation Dynamics reduced-gravity ocean (SPEEDY-RGO) and NEMO models (see their Fig. 3). Therefore, the primary mechanism behind the increase in correlation coefficients between JJAS–Atl3 and NDJF–Niño indices agree with the one reported in previous studies and reviewed in the Introduction (Rodríguez-Fonseca et al. 2009; Polo et al. 2015; Rodríguez-Fonseca et al. 2020).

To identify the reasons for the differences in the Atl3–ENSO teleconnection in AtlSim and CTL (Fig. 4), we look at the differences in the simulated atmospheric and oceanic anomalies during an Atlantic Niño event as represented by the regressions of equatorial anomalies of different variables (averaged between 2°S and 2°N) onto the boreal summer Atl3 index (Fig. 6). During boreal summer, a warming in the equatorial Atlantic SSTs is accompanied by equatorial local positive precipitation anomalies in both simulations (Figs. 6b,e), which

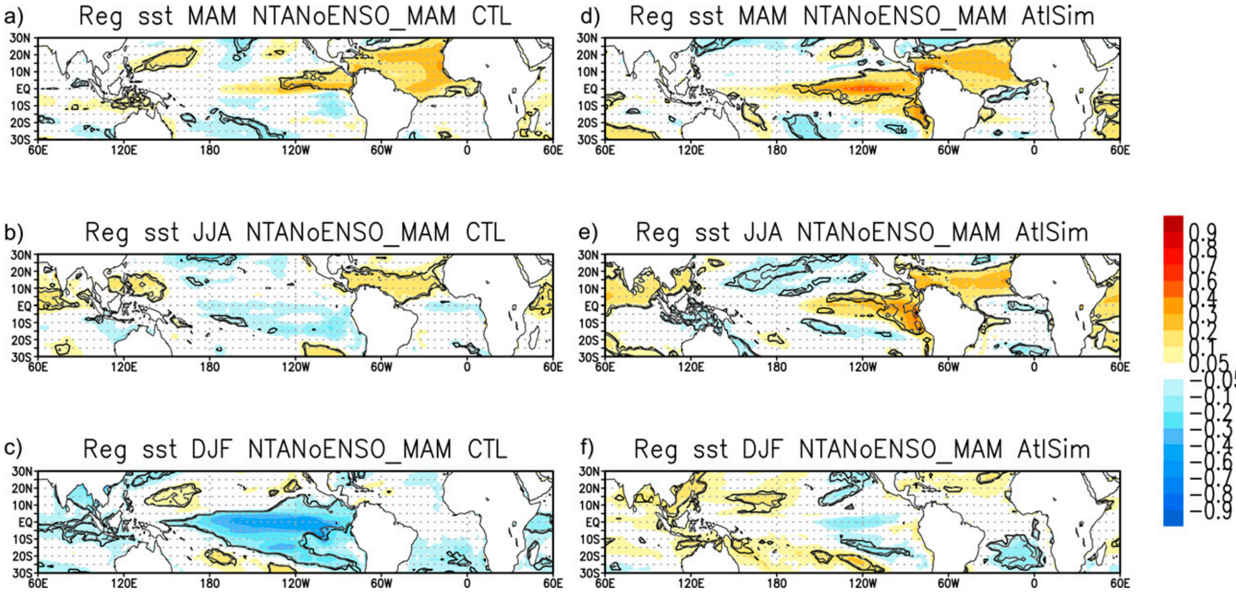

FIG. 7. Regression of the (a),(d) MAM, (b),(e) JJA, and (c),(f) DJF SST (°C) onto the MAM NTA index for CTL simulation in (a)–(c) and AtlSim in (d)–(f). Gray (black) contours show significant correlations at the 95% (90%) level.

are significant between 40°W and 5°E in CTL (Fig. 6b, black line) and between 60°W and 10°E in AtlSim (Fig. 6e, black line). These anomalies appear together with upward motions above (Figs. 6a–d, black lines) and a reduction in the zonal tilt of the Atlantic thermocline, defined as the depth of the maximum vertical temperature gradient (Figs. 6c–f, black lines). However, even though the anomalies of precipitation and vertical velocity (omega) at 500 hPa in the Atlantic sector in CTL are stronger than in AtlSim, they are not able to alter the atmosphere over the equatorial Pacific in boreal summer (Figs. 6a–c, black lines), and thus no equatorial Pacific anomalies develop during the following winter (Figs. 6a–c, blue lines). In contrast, AtlSim shows positive anomalies of omega at 500 hPa in the equatorial Pacific around 120°W, already in JJAS, meaning anomalous downward motions at this location in association with a warm equatorial Atlantic. The westward displacement of the maximum anomalies of precipitation and vertical velocity in AtlSim appears as a plausible cause for the differences in the Pacific response between simulations. This, together with an alteration of the surface winds (Fig. S7, supplementary material), initiates the processes leading to a La Niña response in the following winter. AtlSim winter regressions (Figs. 6d–f, blue lines) show a picture coherent with a Pacific La Niña event. The anomalous descendant motions over the equatorial Pacific are consistent with a negative Southern Oscillation during La Niña events, and there is a reduction of the precipitation in the central and eastern Pacific together with a shoaling of the eastern Pacific thermocline.

Our results suggest, therefore, that a westward extension of the Atlantic Niño in AtlSim could be responsible for the westward shift of the Atlantic deep convection, west of 40°W, which would modify the Atlantic–Pacific Walker circulation and impact the equatorial Pacific. In addition, the experiments suggest that a strengthening of the equatorial ITCZ in AtlSim and a background state of the tropical Pacific that is more sensitive to perturbations in AtlSim than in CTL, due to a shallower thermocline would also help to enhance the teleconnection. These three factors together (westward extension of the Atlantic Niño, strengthening of the equatorial ITCZ and shallower Pacific thermocline) would thus contribute to an enhanced Atl3–Niño-3 connection in AtlSim.

b. NTA–ENSO teleconnection

To examine the teleconnection between the spring north tropical Atlantic and the equatorial Pacific, we follow Ham et al. (2013a) and remove the Niño-3 signal from the detrended and filtered NTA index. CTL shows that positive spring SST anomalies over the NTA tend to be followed by a negative winter ENSO phase (Figs. 7a–c). AtlSim shows a very weak (and nonsignificant) negative correlation between the spring NTA and the following winter equatorial Pacific SST (Fig. 7f). The magnitude of the correlation coefficient between MAM–NTA and DJF–Niño-3 falls from −0.37 (significant at the 95% level) in CTL to −0.04 in AtlSim. In both CTL and AtlSim, the regression patterns of spring-to-winter surface winds and precipitation onto the spring NTA index (Fig. 8) are similar to the ones described in previous works and consistent with the NTA–ENSO teleconnection described by them: That is, a warming in the NTA region produces a Gill-type response that induces a cyclonic circulation in the off-equatorial eastern Pacific and an anticyclonic circulation to the west. The presence of both circulations leads to a surface divergence and cooling in between. It has been shown that this off-equatorial cooling is reinforced by air–sea feedbacks and expands to the equator, triggering a La Niña event

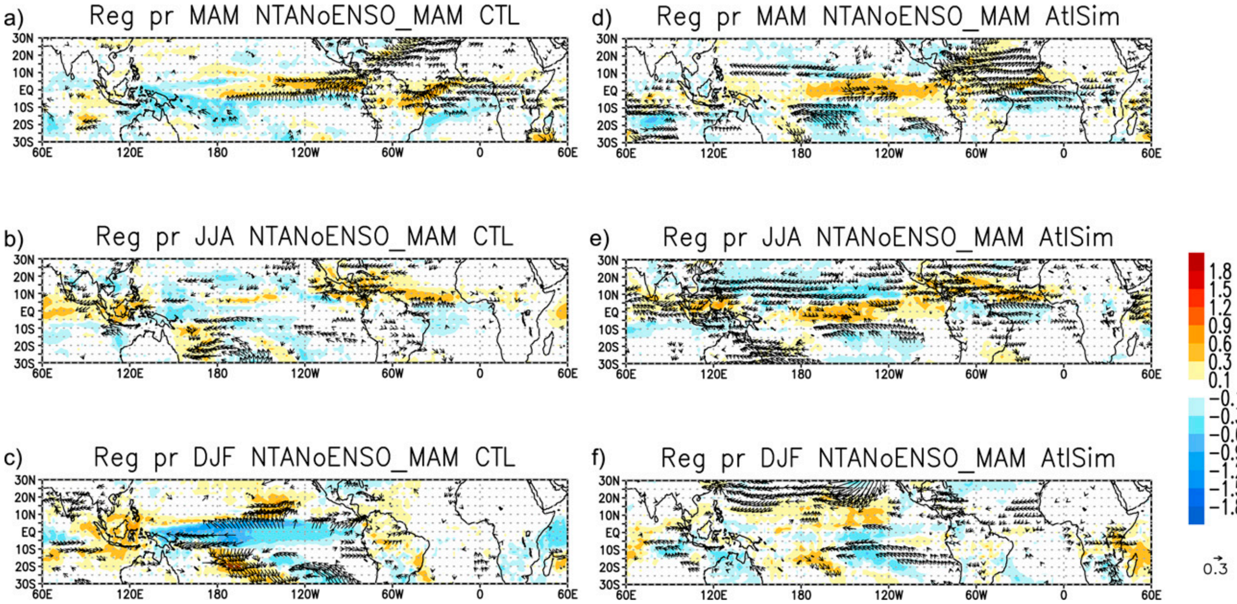

FIG. 8. Regression of the MAM, JJA, and DJF precipitation (mm day^{-1}) (shaded) and surface winds (m s^{-1}) (vectors) onto the MAM NTA index for (a)–(c) CTL and (d)–(f) AtlSim simulations. Only regions with significant differences at the 95% level for surface winds and precipitation are shown.

(Ham et al. 2013b). In CTL, although the response of tropical North Pacific surface winds is weak, it is enough to trigger the teleconnection. Interestingly, the winter Pacific cooling is almost absent in AtlSim, even though the anomalous surface wind pattern associated with an NTA warming is stronger than in CTL.

Wang et al. (2017) related the multidecadal changes in the NTA–Niño-3 correlations to the phase of the AMV and the strength of the Atlantic ITCZ during boreal spring. According to their results, an SST warming in the NTA during positive AMV phases leads to a stronger ITCZ and an enhanced NTA–Niño-3 connection. In our simulation, the change in the Atlantic climatological state resembles a positive AMV, and the precipitation is reinforced in the NTA region (Fig. 1). The thermocline depth is reduced in the central and eastern Pacific (Fig. 1c), the stratification is enhanced there (Fig. S4, supplementary material), and the variability of the SST and thermocline depth is enhanced off the coast of Peru (Figs. 3a,c). Despite all this, the NTA–ENSO connection is weakened. The question now is why is the NTA–Niño-3 connection not enhanced in AtlSim, given that the changes in the Atlantic and Pacific climatological SST and precipitation should favor it? In both simulations, when there is a warming in the NTA, the equatorial eastern Pacific also shows a warming (Figs. 7a,d). A warming of this type could be produced, at least in part, by anomalous westerlies that appear in the region as a response to the NTA warming. In fact, CGCM simulations forced only with NTA anomalies produce a similar signal (Ham et al. 2013a). In AtlSim, these warm anomalies are very strong and persist in boreal summer (Fig. 7e), maybe due to the stronger feedback with the thermocline depth, and lead to a convergence of surface winds in the equatorial Pacific. This convergence is in opposition to the divergence favored by the anomalous winds that appear in the north tropical Pacific as response to the NTA. To explain the stronger response of the equatorial Pacific SST in summer in AtlSim we pose the following hypothesis: the narrowing of the Pacific ITCZ and the enhanced equatorial variability in AtlSim would lead to a concentration of the variability in a narrow equatorial band where the response is enhanced.

The existence of the NTA–ENSO relationship has been questioned in a recent paper (Zhang et al. 2021), in which it is said that the NTA precursor for ENSO is spurious and only appears due to the change in the ENSO frequency from 4 to 2 years. In our results, despite the changes in ENSO frequency go from almost 4 years in CTL to 2.5 years in AtlSim, the NTA–ENSO connection is weakened. Thus, the change in the ENSO frequency cannot account for the change in the NTA–ENSO connection in our simulations. This further suggests that the changes in the climatological mean state of the ITCZ could play a key role in the modulation of the NTA–ENSO teleconnection.

5. Discussion and conclusions

The present paper seeks an increased understanding of the way in which tropical climatology can affect the teleconnections between the tropical Atlantic and the tropical Pacific at interannual time scales. Our emphasis has been on the location of the ITCZ, and we examined the importance of this location in terms of the tropical interannual variability and teleconnections. We also found that changes in the configuration of the Atlantic and Pacific equatorial thermocline depth and ocean stratification are of key importance for such changes. Previous works conducted in different model frameworks have demonstrated links among interhemispheric heating differences and ITCZ displacements, including the formation of a spurious ITZC south of the equator (Hwang and Frierson 2013; Kay et al. 2016). In the context of CGCMs, M16 and the multimodel experiment ETIN-MIP (Kang et al. 2019) looked at the changes in ITCZ location when the model atmosphere was perturbed by reducing the incoming shortwave radiation in full latitude bands. In the present paper we have used the UCLA CGCM, which participated in ETIN-MIP allowing for a contrast with several other models. One asset of this model for the issues addressed here is a high sensitivity to extratropical forcing due to the strong SST–stratocumulus coupling (M16). Our strategy has departed from the studies mentioned earlier in that we perturb the incoming solar radiation in the Southern Atlantic only. This is because the warm bias of CGCMs in the Southern Ocean has the highest values over the Atlantic sector (Wang et al. 2014) and the observational multidecadal changes related to the AMV in the Southern Ocean have maximum loadings over the Atlantic sector (Fig. S1, supplementary material). Moreover, the results of M16 showed a too strong impact of the cooling of an entire latitude band of the Southern Ocean on the equatorial Pacific, where the model performance worsened and the Pacific ITCZ shifted northward. Conversely, in AtlSim, although the equatorial Pacific SSTs are too warm compared to observations, the equatorial precipitation is enhanced in a narrower band around the equator, which enhances the tropical teleconnections. Our results show a strong tropical response to the reduction of incoming radiation in the southern extratropics of the Atlantic sector. In reference to CTL, the tropical Atlantic SSTs in the perturbed simulation are cooler in the Southern Hemisphere and warmer in the Northern Hemisphere. This interhemispheric SST gradient influences the location and strength of the Atlantic ITCZ, which weakens strongly in the south and increases north of the equator. The region of maximum precipitation in the Atlantic sector shifts slightly from 4° to 6°N, resulting in a closer agreement between the simulation and the observations. The reduction of precipitation in the southern tropical Atlantic goes along with a local strengthening of the trade winds (Fig. S3, supplementary material). Moreover, the convergence increases at low levels over the western equatorial Atlantic, where the thermocline steepens and ocean–atmosphere coupling is enhanced. These changes lead to a westward extension of the SST anomalies associated with the Atlantic Niño mode. This results in a westward shift of the anomalous deep convection during an Atlantic Niño, increasing its ability to remotely impact the central equatorial Pacific in boreal summer and to trigger the development of a La Niña event in the following winter. Also, in reference to CTL, the climatology of the tropical Atlantic in AtlSim shows a configuration resembling the *positive* AMV phase.

Based on the observations, Martín-Rey et al. (2018) found similar climatological features in association with a westward extension of the Atlantic Niño. However, the observed changes in the climatological mean state exhibit a reinforcement of the northern trades in the equatorial Atlantic and the SST differences resemble a *negative* AMV phase. An explanation for this seeming discrepancy between observations and simulations is the difference between model and observations in the location of the Atlantic ITCZ, which is far too strong in the south-tropical Atlantic in CTL. The connection between the Atlantic and Pacific Niños seems to occur when the Atlantic ITCZ is located near the equator and equatorial variability is enhanced. In the observations this is achieved by a negative AMV that produces a southward displacement of the ITCZ. In the model it is a positive AMV that leads to a reduction of the spurious precipitation south of the equator, enhancing equatorial dynamics. In both cases, the equatorial variability is enhanced when the ITCZ concentrates equatorward.

In the equatorial Pacific, the AtlSim climatology in reference to CTL shows an El Niño like configuration. The warming in the eastern equatorial Pacific leads to a narrowing of the ITCZ, an increase in the equatorial Pacific vertical stratification and a shallowing of the thermocline in the central and western parts of this ocean. We argue that this configuration makes the equatorial Pacific more sensitive to atmospheric perturbations, enhancing the equatorial Atlantic–Pacific connection. To understand the origin of the eastern tropical Pacific warming in AtlSim (Fig. 1a), which is opposite to the response expected to follow a positive AMV configuration (Ruprich-Robert et al. 2021), we look at the results just after the model integration starts and find that positive SST anomalies can be clearly seen in the eastern southern tropical Pacific almost from the beginning of the simulation (not shown). From this region, the SSTs spread to the deep tropics possibly due to ocean advection and atmosphere–ocean feedback as in Ma et al. (1996).

For the Atlantic Niño–ENSO connection, we have found that the idealized extratropical forcing applied in AtlSim leads to a different location of the ITCZ and a different configuration of the Atlantic equatorial mode, which seems to be related to an enhancement of the connection in reference to CTL. AtlSim results suggest that several factors can contribute to this enhancement: 1) a westward displacement of the perturbations of atmospheric convection due to the Atlantic Niño, produced by enhanced equatorial winds that lead to a stronger variability in the western part of the Atlantic basin; 2) a strengthened equatorial ITCZ; and 3) an equatorial Pacific thermocline more variable and shallower in the west that makes the Pacific Ocean more sensitive to atmospheric perturbations.

In contrast, the NTA–ENSO teleconnection appears to be stronger in CTL than in AtlSim. The correlation between MAM–NTA and DJF–Niño-3 in CTL is −0.37 and significant at the 95% level. The correlation in AtlSim is −0.04 and not statistically significant even though the mechanisms at work for the teleconnection also appear in this simulation. The lack of response of the equatorial Pacific to the NTA in AtlSim can be a result of the competition between the surface divergence in the equatorial Pacific favored by the NTA warming, and the surface convergence due to the presence of warm SST anomalies over the ENSO region. Previous studies have shown a temporal alternation of Atl3–ENSO and NTA–ENSO (Wang et al. 2017; Rodríguez-Fonseca et al. 2020), it is possible that the weakening in the NTA–ENSO connection in AtlSim is produced by the enhancement of the equatorial dynamics in that simulation, due to a more equatorial ITCZ.

A possible two-way interbasin connection, in which Pacific anomalies consistent with a multiyear ENSO influence the equatorial Atlantic wind in boreal spring (Tokinaga et al. 2019) and the location of the Atlantic ITCZ (Rodrigues et al. 2011) cannot be ruled out. Nevertheless, the methodology applied in this work and the results obtained suggest that the main effect the equatorial Pacific can have on the equatorial Atlantic in spring has been removed: the precipitation, surface wind and SST anomalies associated with the Atlantic Niño in boreal summer in AtlSim do not resemble those shown by Tokinaga et al. (2019).

In summary, our results suggest that the representation of the tropical teleconnections between the Atlantic and Pacific basins can be strongly influenced not only by the location of the ITCZ and the regions of maximum convergence, but also through the modification of the climatology of the equatorial Atlantic and Pacific oceanic conditions. In addition, these factors could produce changes in the interannual modes of variability in the tropical oceans, as well as in the interannual tropical teleconnections. Thus, our results suggest that looking at the slowly varying patterns of the climate system can help us understand changes in the interannual teleconnections at decadal scales.

Although the results of this assessment are encouraging, the possibility that longer runs are required for a more definitive answer cannot be entirely ruled out because the presence of low-frequency tropical variability makes it difficult to separate the forced signal. From this viewpoint, our findings can be taken as a potential explanation for the long-term changes in the tropical basin interactions, as well as a new methodology that can be exploited in the future to examine the issue of tropical interbasin teleconnections with longer simulations or even with intercomparison exercises and community efforts with several GCMs.

Acknowledgments. This research was funded by the FP7-PREFACE project (Grant Agreement 603521), the H2020 project TRIATLAS (Grant Agreement 817578), and the Spanish Ministry of Economy and Competitiveness project PRE4CAST (CGL2017-86415-R). Model simulations have been performed un the computation cluster EOLO, funded by the International Campus of Excellence of Moncloa (UCM). The authors are thankful to the three anonymous reviewers whose comments have led to an improvement of the manuscript and to the editor who has helped throughout the publication process.

Data availability statement. Model output is available upon request to the main author.

REFERENCES

Adam, O., T. Schneider, and F. Brient, 2018: Regional and seasonal variations of the double-ITCZ bias in CMIP5 models. *Climate Dyn.*, **51**, 101–117, https://doi.org/10.1007/s00382-017-3909-1.

Adames, Á. F., and J. M. Wallace, 2017: On the tropical atmospheric signature of El Niño. *J. Atmos. Sci.*, **74**, 1923–1939, https://doi.org/10.1175/JAS-D-16-0309.1.

An, S. I., and B. Wang, 2000: Interdecadal change of the structure of the ENSO mode and its impact on the ENSO frequency. *J. Climate*, **13**, 2044–2055, https://doi.org/10.1175/1520-0442(2000)013<2044:ICOTSO>2.0.CO;2.

——, C. Wang, and C. R. Mechoso, 2020: Teleconnections in the atmosphere. *Interacting Climates of Ocean Basins, Observations, Mechanisms, Predictability and Impacts*, C. R. Mechoso, Ed., Cambridge University Press, 358 pp.

Bjerknes, J., 1969: Atmospheric teleconnections from the equatorial Pacific. *Mon. Wea. Rev.*, **97**, 163–172, https://doi.org/10.1175/1520-0493(1969)097<0163:ATFTEP>2.3.CO;2.

Broccoli, A. J., K. A. Dahl, and R. J. Stouffer, 2006: Response of the ITCZ to Northern Hemisphere cooling. *Geophys. Res. Lett.*, **33**, L01702, https://doi.org/10.1029/2005GL024546.

Cai, W., and Coauthors, 2019: Pantropical climate interactions. *Science*, **363**, eaav4236, https://doi.org/10.1126/science.aav4236.

Castaño-Tierno, A., E. Mohino, B. Rodríguez-Fonseca, and T. Losada, 2018: Revisiting the CMIP5 thermocline in the equatorial Pacific and Atlantic Oceans. *Geophys. Res. Lett.*, **45**, 12 963–12 971, https://doi.org/10.1029/2018GL079847.

Chiang, J. C., and A. R. Friedman, 2012: Extratropical cooling, interhemispheric thermal gradients, and tropical climate change. *Annu. Rev. Earth Planet. Sci.*, **40**, 383–412, https://doi.org/10.1146/annurev-earth-042711-105545.

——, Y. Kushnir, and A. Giannini, 2002: Deconstructing Atlantic intertropical convergence zone variability: Influence of the local cross-equatorial sea surface temperature gradient and remote forcing from the eastern equatorial Pacific. *J. Geophys. Res.*, **107**, 4004, https://doi.org/10.1029/2000JD000307.

Deppenmeier, A. L., R. J. Haarsma, and W. Hazeleger, 2016: The Bjerknes feedback in the tropical Atlantic in CMIP5 models. *Climate Dyn.*, **47**, 2691–2707, https://doi.org/10.1007/s00382-016-2992-z.

Ding, H., N. S. Keenlyside, and M. Latif, 2012: Impact of the equatorial Atlantic on the El Niño Southern Oscillation. *Climate Dyn.*, **38**, 1965–1972, https://doi.org/10.1007/s00382-011-1097-y.

Dippe, T., J. F. Lübbecke, and R. J. Greatbatch, 2019: A comparison of the Atlantic and Pacific Bjerknes feedbacks: Seasonality, symmetry, and stationarity. *J. Geophys. Res. Oceans*, **124**, 2374–2403, https://doi.org/10.1029/2018JC014700.

Ebisuzaki, W., 1997: A method to estimate the statistical significance of a correlation when the data are serially correlated. *J. Climate*, **10**, 2147–2153, https://doi.org/10.1175/1520-0442(1997)010<2147:AMTETS>2.0.CO;2.

Exarchou, E., P. Ortega, P., B. Rodríguez-Fonseca, T. Losada, I. Polo, and C. Prodhomme, 2021: Impact of equatorial Atlantic variability on ENSO predictive skill. *Nat. Commun.*, **12**, 1612, https://doi.org/10.1038/s41467-021-21857-2.

Fedorov, A. V., and S. G. Philander, 2000: Is El Niño changing? *Science*, **288**, 1997–2002, https://doi.org/10.1126/science.288.5473.1997.

Frauen, C., and D. Dommenget, 2012: Influences of the tropical Indian and Atlantic Oceans on the predictability of ENSO. *Geophys. Res. Lett.*, **39**, L02706, https://doi.org/10.1029/2011GL050520.

Friedman, A. R., Y. T. Hwang, J. C. Chiang, and D. M. Frierson, 2013: Interhemispheric temperature asymmetry over the twentieth century and in future projections. *J. Climate*, **26**, 5419–5433, https://doi.org/10.1175/JCLI-D-12-00525.1.

Green, B., and J. Marshall, 2017: Coupling of trade winds with ocean circulation damps ITCZ shifts. *J. Climate*, **30**, 4395–4411, https://doi.org/10.1175/JCLI-D-16-0818.1.

——, ——, and J. M. Campin, 2019: The 'sticky' ITCZ: Ocean-moderated ITCZ shifts. *Climate Dyn.*, **53**, 1–19, https://doi.org/10.1007/s00382-019-04623-5.

Ham, Y. G., J. S. Kug, J. Y. Park, and F. F. Jin, 2013a: Sea surface temperature in the north tropical Atlantic as a trigger for El Niño/Southern Oscillation events. *Nat. Geosci.*, **6**, 112–116, https://doi.org/10.1038/ngeo1686.

——, ——, and ——, 2013b: Two distinct roles of Atlantic SSTs in ENSO variability: North tropical Atlantic SST and Atlantic Niño. *Geophys. Res. Lett.*, **40**, 4012–4017, https://doi.org/10.1002/grl.50729.

Hu, Z. Z., A. Kumar, H. L. Ren, H. Wang, M. L'Heureux, and F. F. Jin, 2013: Weakened interannual variability in the tropical Pacific Ocean since 2000. *J. Climate*, **26**, 2601–2613, https://doi.org/10.1175/JCLI-D-12-00265.1.

Hwang, Y. T., and D. M. Frierson, 2013: Link between the double-intertropical convergence zone problem and cloud biases over the Southern Ocean. *Proc. Natl. Acad. Sci. USA*, **110**, 4935–4940, https://doi.org/10.1073/pnas.1213302110.

Jansen, M. F., D. Dommenget, and N. Keenlyside, 2009: Tropical atmosphere–ocean interactions in a conceptual framework. *J. Climate*, **22**, 550–567, https://doi.org/10.1175/2008JCLI2243.1.

Kang, S. M., 2020: Extratropical influence on the tropical rainfall distribution. *Curr. Climate Change Rep.*, **6**, 24–36, https://doi.org/10.1007/s40641-020-00154-y.

——, I. M. Held, D. M. Frierson, and M. Zhao, 2008: The response of the ITCZ to extratropical thermal forcing: Idealized slab-ocean experiments with a GCM. *J. Climate*, **21**, 3521–3532, https://doi.org/10.1175/2007JCLI2146.1.

——, D. M. Frierson, and I. M. Held, 2009: The tropical response to extratropical thermal forcing in an idealized GCM: The importance of radiative feedbacks and convective parameterization. *J. Atmos. Sci.*, **66**, 2812–2827, https://doi.org/10.1175/2009JAS2924.1.

——, and Coauthors, 2019: Extratropical–Tropical Interaction Model Intercomparison Project (Etin-Mip): Protocol and initial results. *Bull. Amer. Meteor. Soc.*, **100**, 2589–2606, https://doi.org/10.1175/BAMS-D-18-0301.1.

Kay, J. E., C. Wall, V. Yettella, B. Medeiros, C. Hannay, P. Caldwell, and C. Bitz, 2016: Global climate impacts of fixing the Southern Ocean shortwave radiation bias in the Community Earth System Model (CESM). *J. Climate*, **29**, 4617–4636, https://doi.org/10.1175/JCLI-D-15-0358.1.

Keenlyside, N., Y. Kosaka, N. Vigaud, A. Robertson, Y. Wang, D. Dommenget, J.-J. Luo, and D. Matei, 2020: Basin interactions and predictability. *Interacting Climates of Ocean Basins, Observations, Mechanisms, Predictability and Impacts*, C. R. Mechoso, Ed., Cambridge University Press, 258–292.

Knight, J. R., R. J. Allan, C. K. Folland, M. Vellinga, and M. E. Mann, 2005: A signature of persistent natural thermohaline circulation cycles in observed climate. *Geophys. Res. Lett.*, **32**, L20708, https://doi.org/10.1029/2005GL024233.

Konor, C. S., G. C. Boezio, C. R. Mechoso, and A. Arakawa, 2009: Parameterization of PBL processes in an atmospheric general circulation model: Description and preliminary assessment. *Mon. Wea. Rev.*, **137**, 1061–1082, https://doi.org/10.1175/2008MWR2464.1.

Li, J. L. F., M. Köhler, J. D. Farrara, and C. R. Mechoso, 2002: The impact of stratocumulus cloud radiative properties on surface heat fluxes simulated with a general circulation model. *Mon. Wea. Rev.*, **130**, 1433–1441, https://doi.org/10.1175/1520-0493(2002)130<1433:TIOSCR>2.0.CO;2.

Losada, T., and B. Rodríguez-Fonseca, 2016: Tropical atmospheric response to decadal changes in the Atlantic equatorial mode. *Climate Dyn.*, **47**, 1211–1224, https://doi.org/10.1007/s00382-015-2897-2.

——, ——, I. Polo, S. Janicot, S. Gervois, F. Chauvin, and P. Ruti, 2010: Tropical response to the Atlantic equatorial mode: AGCM multimodel approach. *Climate Dyn.*, **35**, 45–52, https://doi.org/10.1007/s00382-009-0624-6.

Lübbecke, J., B. Rodríguez-Fonseca, I. Richter, M. Martín-Rey, T. Losada, I. Polo, and N. Keenlyside, 2018: Equatorial Atlantic variability—Modes, mechanisms, and global teleconnections. *Wiley Interdiscip. Rev.: Climate Change*, **9**, e527, https://doi.org/10.1002/wcc.527.

Ma, C. C., C. R. Mechoso, A. W. Robertson, and A. Arakawa, 1996: Peruvian stratus clouds and the tropical Pacific circulation: A coupled ocean–atmosphere GCM study. *J. Climate*, **9**, 1635–1645, https://doi.org/10.1175/1520-0442(1996)009<1635:PSCATT>2.0.CO;2.

Ma, H. Y., H. Xiao, C. R. Mechoso, and Y. Xue, 2013: Sensitivity of global tropical climate to land surface processes: Mean state and interannual variability. *J. Climate*, **26**, 1818–1837, https://doi.org/10.1175/JCLI-D-12-00142.1.

Marshall, J., and Coauthors, 1997: A finite-volume, incompressible Navier Stokes model for studies of the ocean on parallel computers. *J. Geophys. Res.*, **102**, 5753–5766, https://doi.org/10.1029/96JC02775.

Martín-Rey, M., B. Rodríguez-Fonseca, I. Polo, and F. Kucharski, 2014: On the Atlantic–Pacific Niños connection: A multidecadal modulated mode. *Climate Dyn.*, **43**, 3163–3178, https://doi.org/10.1007/s00382-014-2305-3.

——, ——, and ——, 2015: Atlantic opportunities for ENSO prediction. *Geophys. Res. Lett.*, **42**, 6802–6810, https://doi.org/10.1002/2015GL065062.

——, I. Polo, B. Rodríguez-Fonseca, T. Losada, and A. Lazar, 2018: Is there evidence of changes in tropical Atlantic variability modes under AMO phases in the observational record? *J. Climate*, **31**, 515–536, https://doi.org/10.1175/JCLI-D-16-0459.1.

——, ——, ——, A. Lazar, and T. Losada, 2019: Ocean dynamics shapes the structure and timing of Atlantic equatorial modes. *J. Geophys. Res. Oceans*, **124**, 7529–7544, https://doi.org/10.1029/2019JC015030.

McGee, D., E. Moreno-Chamarro, B. Green, J. Marshall, E. Galbraith, and L. Bradtmiller, 2018: Hemispherically asymmetric trade wind changes as signatures of past ITCZ shifts. *Quat. Sci. Rev.*, **180**, 214–228, https://doi.org/10.1016/j.quascirev.2017.11.020.

Mechoso, C. R., and Coauthors, 1995: The seasonal cycle over the tropical Pacific in coupled ocean–atmosphere general circulation models. *Mon. Wea. Rev.*, **123**, 2825–2838, https://doi.org/10.1175/1520-0493(1995)123<2825:TSCOTT>2.0.CO;2.

——, J.-Y. Yu, and A. Arakawa, 2000: A coupled GCM pilgrimage: From climate catastrophe to ENSO simulations. *General Circulation Model Development: Past, Present and Future*, D. A. Randall, Ed., Academic Press, 539–575.

——, and Coauthors, 2016: Can reducing the incoming energy flux over the Southern Ocean in a CGCM improve its simulation of tropical climate? *Geophys. Res. Lett.*, **43**, 11 057–11 063, https://doi.org/10.1002/2016GL071150.

Mohino, E., B. Rodríguez-Fonseca, C. R. Mechoso, T. Losada, and I. Polo, 2019: Relationships among intermodel spread and biases in tropical Atlantic sea surface temperatures. *J. Climate*, **32**, 3615–3635, https://doi.org/10.1175/JCLI-D-18-0846.1.

Neelin, J. D., 2010: *Climate Change and Climate Modeling*. Cambridge University Press, 304 pp.

Oueslati, B., and G. Bellon, 2015: The double ITCZ bias in CMIP5 models: Interaction between SST, large-scale circulation and precipitation. *Climate Dyn.*, **44**, 585–607, https://doi.org/10.1007/s00382-015-2468-6.

Polo, I., M. Martin-Rey, B. Rodriguez-Fonseca, F. Kucharski, and C. R. Mechoso, 2015: Processes in the Pacific La Niña onset triggered by the Atlantic Niño. *Climate Dyn.*, **44**, 115–131, https://doi.org/10.1007/s00382-014-2354-7.

Richter, I., 2015: Climate model biases in the eastern tropical oceans: Causes, impacts and ways forward. *Wiley Interdiscip. Rev.: Climate Change*, **6**, 345–358, https://doi.org/10.1002/wcc.338.

——, S. P. Xie, S. K. Behera, T. Doi, and Y. Masumoto, 2014: Equatorial Atlantic variability and its relation to mean state biases in CMIP5. *Climate Dyn.*, **42**, 171–188, https://doi.org/10.1007/s00382-012-1624-5.

Rodrigues, R. R., R. J. Haarsma, E. J. Campos, and T. Ambrizzi, 2011: The impacts of inter–El Niño variability on the tropical Atlantic and northeast Brazil climate. *J. Climate*, **24**, 3402–3422, https://doi.org/10.1175/2011JCLI3983.1.

Rodríguez-Fonseca, B., I. Polo, J. García-Serrano, T. Losada, E. Mohino, C. R. Mechoso, and F. Kucharski, 2009: Are Atlantic Niños enhancing Pacific ENSO events in recent decades? *Geophys. Res. Lett.*, **36**, L20705, https://doi.org/10.1029/2009GL040048.

——, Y.-G. Ham, S.-K. Lee, M. Martín-Rey, I. Polo, and R. Rodrigues, 2020: Interacting interannual variability of the Pacific and Atlantic Oceans. *Interacting Climates of Ocean Basins, Observations, Mechanisms, Predictability and Impacts*, C. R. Mechoso, Ed., Cambridge University Press, 120–152.

Ruprich-Robert, Y., and Coauthors, 2021: Impacts of Atlantic multidecadal variability on the tropical Pacific: A multi-model study. *npj Climate Atmos. Sci.*, **4**, 33, https://doi.org/10.1038/s41612-021-00188-5.

Tian, B., and Dong, X., 2020: The double-ITCZ bias in CMIP3, CMIP5, and CMIP6 models based on annual mean precipitation. *Geophys. Res. Lett.*, **47**, e2020GL087232, https://doi.org/10.1029/2020GL087232.

Tokinaga, H., I. Richter, and Y. Kosaka, 2019: ENSO influence on the Atlantic Niño, revisited: Multi-year versus single-year ENSO events. *J. Climate*, **32**, 4585–4600, https://doi.org/10.1175/JCLI-D-18-0683.1.

Wang, B., and Coauthors, 2019: Historical change of El Niño properties sheds light on future changes of extreme El Niño. *Proc. Natl. Acad. Sci. USA*, **116**, 22 512–22 517, https://doi.org/10.1073/pnas.1911130116.

Wang, C., L. Zhang, S. K. Lee, L. Wu, and C. R. Mechoso, 2014: A global perspective on CMIP5 climate model biases. *Nat. Climate Change*, **4**, 201–205, https://doi.org/10.1038/nclimate2118.

Wang, L., J. Y. Yu, and H. Paek, 2017: Enhanced biennial variability in the Pacific due to Atlantic capacitor effect. *Nat. Commun.*, **8**, 14887, https://doi.org/10.1038/ncomms14887.

White, R. H., A. A. McFarlane, D. M. Frierson, S. M. Kang, Y. Shin, and M. Friedman, 2018: Tropical precipitation and cross-equatorial heat transport in response to localized heating: Basin and hemisphere dependence. *Geophys. Res. Lett.*, **45**, 11–949, https://doi.org/10.1029/2018GL078781.

Xiang, B., M. Zhao, Y. Ming, W. Yu, and S. M. Kang, 2018: Contrasting impacts of radiative forcing in the Southern Ocean versus southern tropics on ITCZ position and energy transport in one GFDL climate model. *J. Climate*, **31**, 5609–5628, https://doi.org/10.1175/JCLI-D-17-0566.1.

Xie, P., and P. A. Arkin, 1997: Global precipitation: A 17-year monthly analysis based on gauge observations, satellite estimates, and numerical model outputs. *Bull. Amer. Meteor. Soc.*, **78**, 2539–2558, https://doi.org/10.1175/1520-0477(1997)078<2539:GPAYMA>2.0.CO;2.

Xue, Y., P. J. Sellers, J. L. Kinter, and J. Shukla, 1991: A simplified biosphere model for global climate studies. *J. Climate*, **4**, 345–364, https://doi.org/10.1175/1520-0442(1991)004<0345:ASBMFG>2.0.CO;2.

Yu, J., and C. R. Mechoso, 1999: Links between annual variations of Peruvian stratocumulus clouds and of SST in the eastern equatorial Pacific. *J. Climate*, **12**, 3305–3318, https://doi.org/10.1175/1520-0442(1999)012<3305:LBAVOP>2.0.CO;2.

Yu, S., and M. S. Pritchard, 2019: A strong role for the AMOC in partitioning global energy transport and shifting ITCZ position in response to latitudinally discrete solar forcing in CESM1.2. *J. Climate*, **32**, 2207–2226, https://doi.org/10.1175/JCLI-D-18-0360.1.

Zebiak, S. E., 1993: Air–sea interaction in the equatorial Atlantic region. *J. Climate*, **6**, 1567–1586, https://doi.org/10.1175/1520-0442(1993)006<1567:AIITEA>2.0.CO;2.

Zhang, W., G. Villarini, L. Slater, G. A. Vecchi, and A. A. Bradley, 2017: Improved ENSO forecasting using Bayesian updating and the North American Multimodel Ensemble (NMME). *J. Climate*, **30**, 9007–9025, https://doi.org/10.1175/JCLI-D-17-0073.1.

——, F. Jiang, M. F. Stuecker, F. F. Jin, and A. Timmermann, 2021: Spurious North tropical Atlantic precursors to El Niño. *Nat. Commun.*, **12**, 3096, https://doi.org/10.1038/s41467-021-23411-6.

Zhu, J., A. Kumar, and B. Huang, 2015: The relationship between thermocline depth and SST anomalies in the eastern equatorial Pacific: Seasonality and decadal variations. *Geophys. Res. Lett.*, **42**, 4507–4515, https://doi.org/10.1002/2015GL064220.